한국지반공학회논문집 제27권 2호 2011년 2월 pp. 35 ~ 42

Field Behavior of Residual Stresses on Rock Socketed Drilled Shafts

암반에 근입된 현장타설말뚝에 작용하는 잔류응력의 현장거동

Nam, Moon S.[1] 남 문 석

요 지

현장타설말뚝의 하중전이분석 시, 말뚝에 작용하는 잔류응력은 종종 무시되어 왔다. 그러나 말뚝에 작용하는 초기 하중를 무시함에 따라서 분석된 하중전이거동이 실제 하중전이거동과 상이하게 나타나는 결과를 초래하기도 한다. 이러한 현장타설말뚝에 작용하는 잔류응력은 콘크리트의 수축/팽창 또는 지반의 특성에 영향을 받는 것으로 몇몇의 연구결과에 의하여 나타났다. 본 연구에서는 암반에 근입된 현장타설말뚝을 시험시공하여 잔류응력을 측정하고 분석하였으며, 이에 따른 잔류응력에 미치는 요소들에 대하여 검토 분석하였다.

Abstract

The residual stress on drilled shafts is often neglected. Neglect of the existence of locked-in loads in the shaft is the main reason for conclusions of instrumented tests which suggest that shaft resistance is smaller when the shaft is loaded in tension than when it is loaded in compression. A few researchers studied the residual stress and mentioned that the residual stress is influenced by either the physical expansion/contraction of concrete during the curing or site stratigraphy. In this study, field measurements of residual stress on test shafts were conducted and the factors influencing the residual stress were figured out.

Keywords : Concrete, Field measurements, Residual stress, Rock socketed drilled shafts, Site stratigraphy

1. Introduction

Load tests on drilled shafts sometimes include instrumentation for determining the load distribution. Most measurements are analyzed from the assumption that the "zero readings", which are the readings taken at "zero" time also have registered "zero" load. It neglects the existence of locked-in loads (residual load) in the shaft. Neglect of the residual load distribution is also the main reason for conclusions of instrumented tests which suggest that shaft resistance is smaller when the shaft is loaded in tension than when it is loaded in compression (Fellenius, 2002).

Hayes and Simmons (2002) proposed that the physical expansion and contraction of concrete in the drilled shaft during the curing period result in significant residual stress. However, Kim et al. (2004) proposed the other aspect on the residual stress, that is, the residual stress in the specific augered cast-in-place piles installed in typical Texas Gulf Coast layered with clay and sand strata was tensile due to expansion of the clay soils and concluded that the residual behavior is influenced by site stratigraphy.

1 정회원, 한국도로공사 도로교통연구원 책임연구원 (Member, Senior Researcher, Expressway & Transportation Research Institute, Korea Expressway Corp., moonsnam@gmail.com, 교신저자)

* 본 논문에 대한 토의를 원하는 회원은 2011년 8월 31일까지 그 내용을 학회로 보내주시기 바랍니다. 저자의 검토 내용과 함께 논문집에 게재하여 드립니다.

This paper presents field measurements of residual stress on test shafts, and then figures out the factors affecting the residual stress.

2. Field Test Sites and Test Shafts

In order to construct test shafts and measure residual stresses, a total of three test sites [Hampton (HT), Denton Tap (DT), and Rowlett Creek (RC)] were selected in north central Texas, USA. The soft rock formations in this area are upper Cretaceous formations, which includes the Eagle Ford (clay shale) and Austin (limestone) formations. The sites selected for the current study consisted of two clay shale sites (HT and DT) and one limestone sites (RC).

In order to investigate engineering properties, compression tests [UU triaxial testing for clay shale samples (ASTM 2664), unconfined compression testing for limestone samples (ASTM 2938)] were performed in the laboratory and the results are shown in Figure 1. Based on the site investigation and laboratory tests, the test shafts were designed using Osterberg cells with reaction shafts as shown in Figure 1. Also, three test shafts were instrumented by using calibrated vibrating wire sister bars (Geokon Model 4911) to measure residual stress in the test shafts and the reaction shafts. Further information for the test site is in Nam (2004).

3. Instrumentations

The vibrating wire sister bar consists of a strain meter body and two 594-mm long sections of No. 4 deformed reinforcing bars which are welded at each end of the strain meter body. In the strain meter body, a strain gage, thermistor and electromagnetic coil are contained. Since each vibrating wire sister bar was calibrated by the manufacturer using the linear regression method and had its own gage factor, gage factors were applied in estimating the strains in test shafts.

A total of 12 vibrating wire sister bars were used at four strain measuring points along the length of the test shaft and two vibrating wire sister bars were horizontally installed at concrete curing monitoring points across the rebar cage for the HT site (Figure 2). The concrete curing monitoring point was used to monitor the expansion or contraction of concrete during its curing. The test shaft had two strain measuring points, 8.2 m and 9.2 m below grade and two concrete curing monitoring points, 9.0 m and 9.1 m below grade. At the strain measuring points in the test shaft, four vibrating wire sister bars were attached at each point with 90, 180, 270, and 360 degree positions. The two concrete curing monitoring points were perpendicular with each other and one vibrating wire sister bar was attached at each point.

In the DT site, a total of 20 vibrating wire sister bars

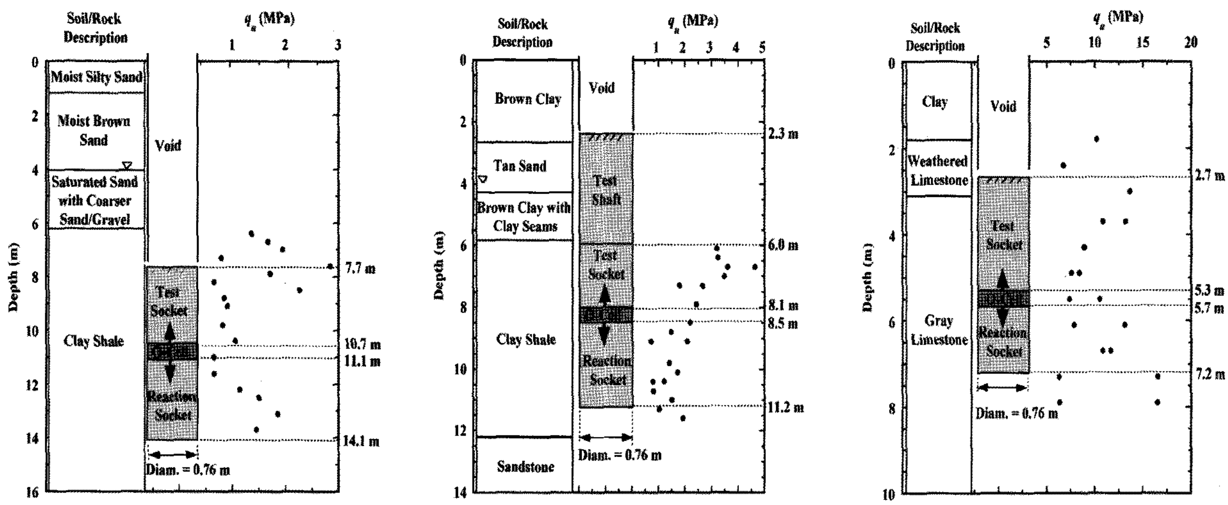

(a) HT (b) DT (c) RC

Fig. 1. Geomaterial Properties and Test Shafts

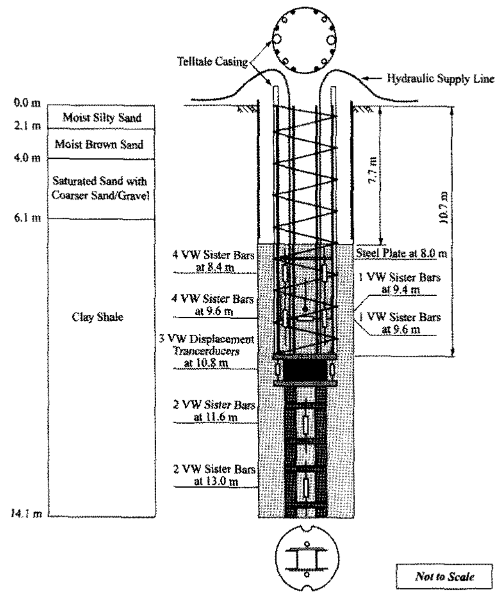

Fig. 2. Instrumentations on HT Site

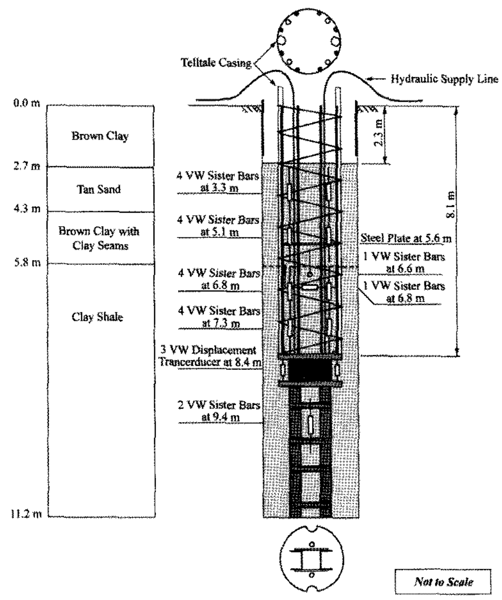

Fig. 3. Instrumentations for DT Site

were used at six strain measuring points along the length of the test shaft and two vibrating wire sister bars were horizontally installed at concrete curing monitoring points across the rebar cage (Figure 3). The test shaft had four strain measuring points, 3.3 m, 5.2 m, 6.8 m and 7.2 m below grade and two concrete curing monitoring points, 6.6 m and 6.7 m below grade. At the strain measuring points in the test shaft, four vibrating wire sister bars were attached at each point with 90, 180, 270, and 360 degree positions. The two concrete curing monitoring points were perpendicular with each other and one vibrating

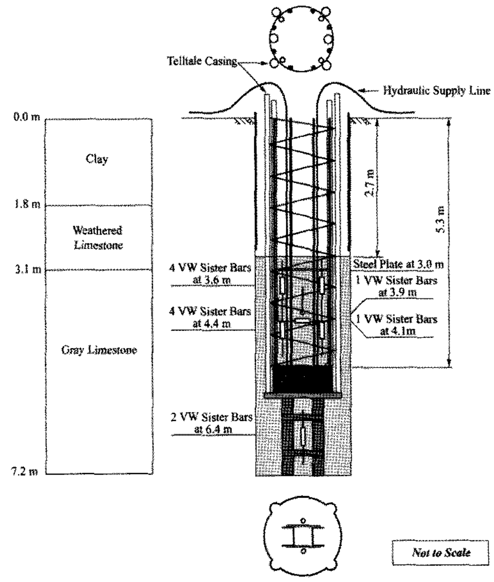

Fig. 4. Instrumentations for RC Site

wire sister bar was attached at the each point.

In the RC site, a total of 10 vibrating wire sister bars were instrumented at three strain measuring points along the length of the test shaft and two vibrating wire sister bars were horizontally installed at concrete curing monitoring points across the rebar cage (Figure 4). The test shaft had two strain measuring points, 3.6 m and 4.3 m below grade and two concrete curing monitoring points, 3.9 m and 4.0 m below grade. At the strain measuring points in the test shaft, four vibrating wire sister bars were attached at each point with 90, 180, 270, and 360 degree positions. The two concrete curing monitoring points were perpendicular with each other and one vibrating wire sister bar was attached at each point. The reaction shaft had only one strain measuring point, 6.4 m below grade, along the twin steel channels.

In order to avoid damages of sister bars at the concrete curing monitoring point due to direct hitting by concrete dropping, a steel plate (about 50 mm wide × 545 mm long × 6.4 mm thick) was welded at the rebar cage about 1.0 m above the sister bar in each test shaft.

4. Residual Stress Measurements

In order to estimate residual stress on test shafts during concrete curing, sister bar gauges at various levels were monitored until the day of load tests (curing period, about

50-day after casting). Initial strain readings were made just before concrete was placed. Temperatures and strains were measured from vibrating wire sister bars in each test shaft during the curing period. Figures 5 to 7 show temperature histories of the test shafts for test sites during the curing period. Temperatures were significantly rose up to 38.6℃ around two days after casting due to the heat of hydration, and then rapidly dropped for 15 days. After 15 days, they had stabilized. The behavior of temperature histories appeared to be consistent for all test sites.

For reducing sister bar readings that will be converted to stresses by multiplying elastic modului to strains from sister bar readings, concrete cylindrical specimens (diameter = 152 mm and height = 304.8 mm) were taken from the fileds and then tested by compression testing machines at various curing times of the concrete. A total of six compression tests for each site were conducted at one (one sample), 13 (two samples) and 49 days old (load test day, three samples) for the HT site, two (one sample), 11 (two samples) and 48 days old (load test day, three samples) for the DT site, and two (one sample), 15 (two samples) and 51 days old (load test day, three samples) for RC site after concrete placed. The compressive strengths, f_c' according to curing ages is shown in Figure 8, and the values of f_c' for each site on the day of load test were estimated by averaging three samples and the values were 36.0 MPa for the HT site, 40.2 MPa for the DT, and 32.3 MPa for the RC site as summarized in Table 1.

Since the compressive tests at intermediate times (about two and 14 days after casting) were performed to assure their failures without strain-gauged, concrete moduli (E_c) at intermediate times were estimated by multiplying the ratio of E_c / f_c' at the day of the load test to measured intermediate compressive strengths (f_c') on the assumption that E_c / f_c' at the day of the load test was nearly constant over the curing time at each site. The ratios E_c / f_c' at the day of the load test were computed in Table 1. Thereafter,

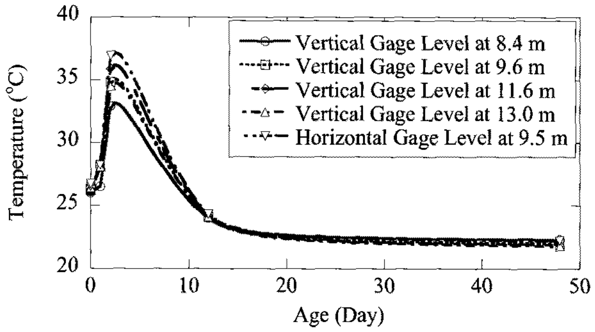

Fig. 5. Temperature History During Curing Period for HT Site

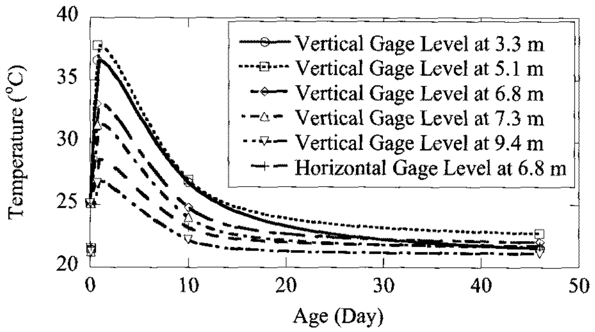

Fig. 6. Temperature History During Curing Period for DT Site

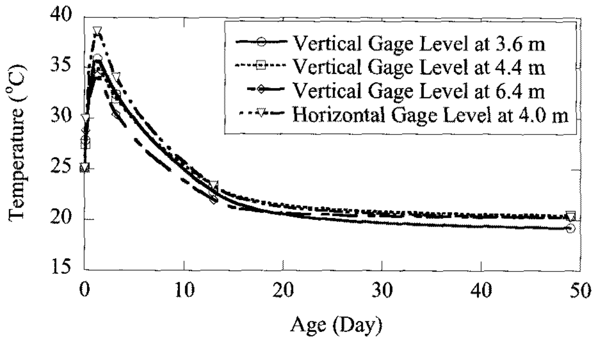

Fig. 7. Temperature History During Curing Period for RC Site

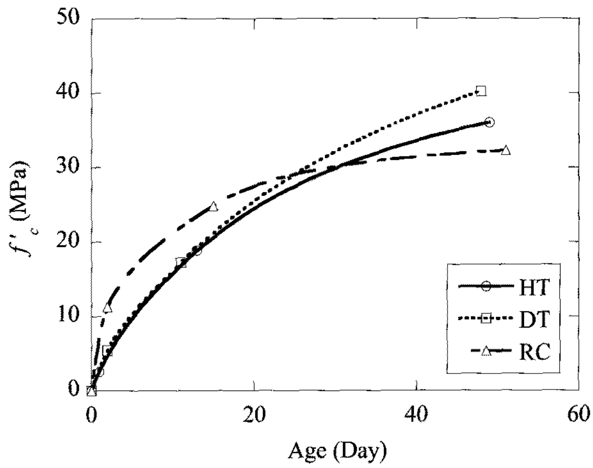

Fig. 8. Concrete Compressive Strengths at Various Curing Ages

Table 1. Ratios of E_c / f_c' at Day of Load Test for Test Sites

	HT	DT	RC
E_c (MPa)	25751	29213	43425
f_c' (MPa)	36	40	32
E_c / f_c'	716	726	1344

E_c values at intermediate times were estimated by using the ratio E_c / f_c' at the day of the load test, as shown in Figure 9. These E_c values at intermediate times will be applied to convert strains at various levels incrementally in time (Figure 9) to residual stresses (σ) during curing period by multiplying with strains (Equation 1). This method of estimating moduli was subjected to limitations and error margins.

$$\sigma = \sum_{t=0}^{t=t_{max}} \left(\varepsilon_t - \varepsilon_{t-1}\right)\left(\frac{E_{ct-1} + E_{ct}}{2}\right) \tag{1}$$

It is noted that the difference of E_c / f_c' between the RC site and the other 2 sites (HT and DT) in Table 1 is due to differences of concrete placing time and curing environment at each site.

According to the procedure, the strain and stress at each level of sister bar gauges were computed. Figure 10 and 11 show strain and stress histories at the HT site for the curing period, respectively. Both strains and stresses rapidly increased to the compressive zone around two days after casting due to the shrinkage of concrete, and then had suddenly dropped to the tensile zone for 12 days except two sister bars installed at 9.5 m. After 12 days after casting, strains and stresses at levels of 11.6 and 13.0 m (clay shale) gradually decreased. However, strains and stresses at levels of 8.4, 9.5 and 9.6 m (clay shale) gradually increased after 12 days.

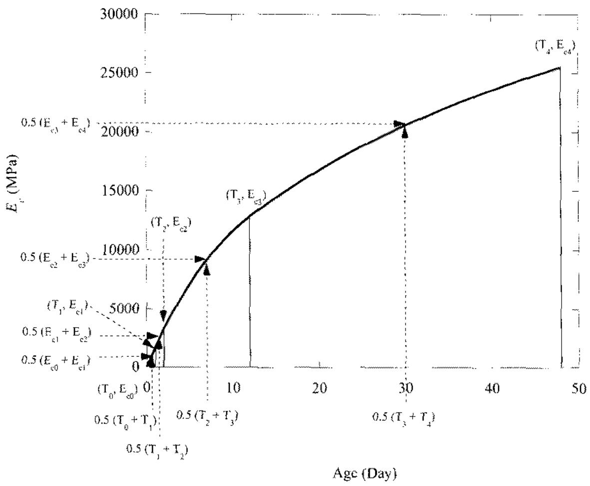

Fig. 9. Estimated Elastic Modulus Against Concrete Curing Time for HT Site

The residual behavior at each level at the DT site is shown in Figures 12 and 13. The residual behaviors at 3.3 and 5.1 m (overburden soil) increased to the compressive zone for one day after casting due to the shrinkage of concrete, and then gradually increased for 10 days, were finally stabilized after 10 days. The residual behavior at 6.8 m (both vertical and horizontal gages in clay shale) rapidly increased to the compressive zone for one day after casting due to the shrinkage of concrete, and then gradually increased after one day. The residual behaviors at 7.3 and 9.5 m (clay shale) increased to the compressive zone around one day after casting due to the shrinkage of concrete, and then suddenly dropped to the tensile zone for 10 days. After 10 days, the residual behavior gradually increased along with curing time.

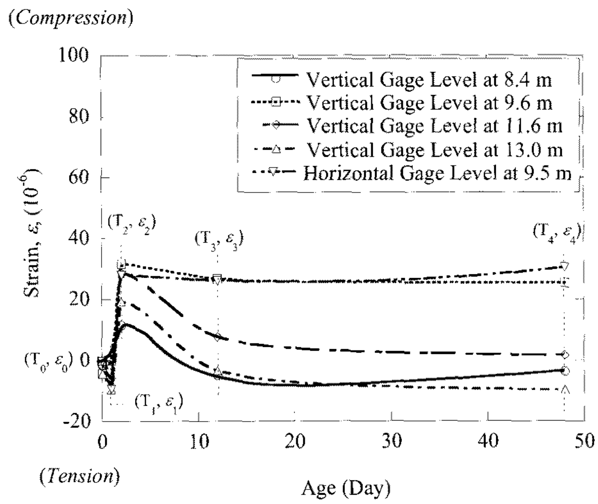

Fig. 10. Strain History for HT Site

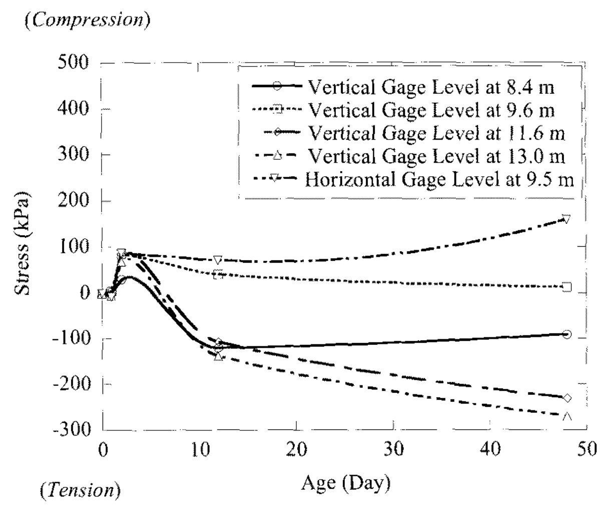

Fig. 11. Residual Stresses for HT Site

The residual behavior at each level at the Rowlett Creek site is shown in Figures 14 and 15. The residual behaviors at 3.6, 4.0, and 4.4 m (limestone) rapidly increased to the compressive zone for two day after casting due to the shrinkage of concrete, and then gradually dropped to the tensile zone after two days. However, the residual behavior at 6.4 m (limestone) rapidly dropped for 13 days, and then picked up to the compressive zone and gradually increased after 13 days after casting.

Figures 16 to 18 show residual stresses (from vertically installed sister bars) and normal stresses (from horizontally installed sister bars) developed just before the day of the load test (about 50 days) along with depth. Residual stresses at the HT site were negative stresses that represented the swelling of the shaft along with the shaft length. The normal stress at the HT site was a positive stress that represented the shrinkage of the shaft along with the shaft diameter. Both residual and normal stresses at the DT site were a positive stress that represented the shrinkage of the shaft in both directions. It was noted that the residual stress behavior in the DT site was different from that in the HT site, unlike normal stresses. It might have been caused by the confing effect of the shaft weight installed in overburden soils, which influenced compressive stresses to the socket. Both residual and normal stresses at the RC site were negative stresses that represented the swelling of the shaft in both directions.

These negative and positive normal stresses can be

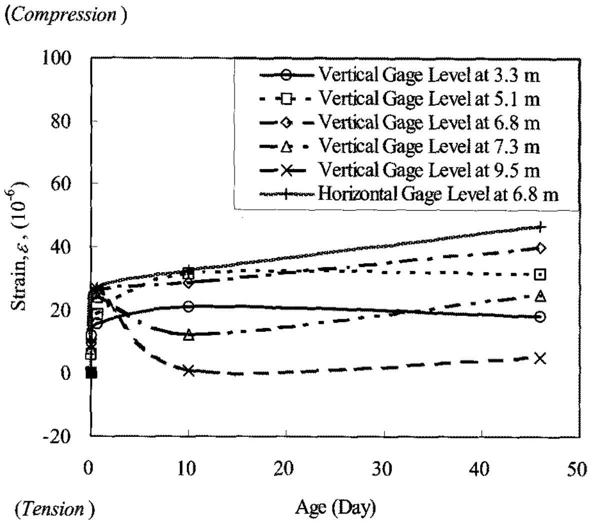

Fig. 12. Strain History for DT Site

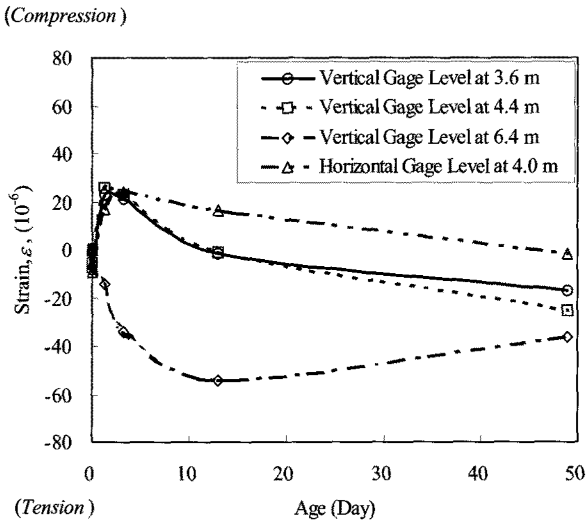

Fig. 14. Strain History for RC Site

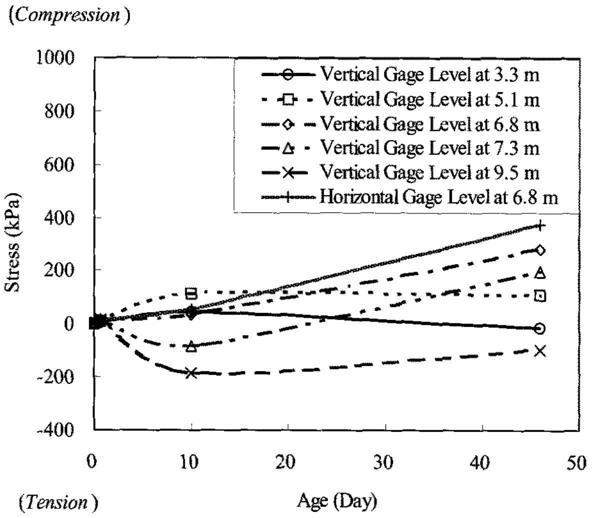

Fig. 13. Residual Stresses for DT Site

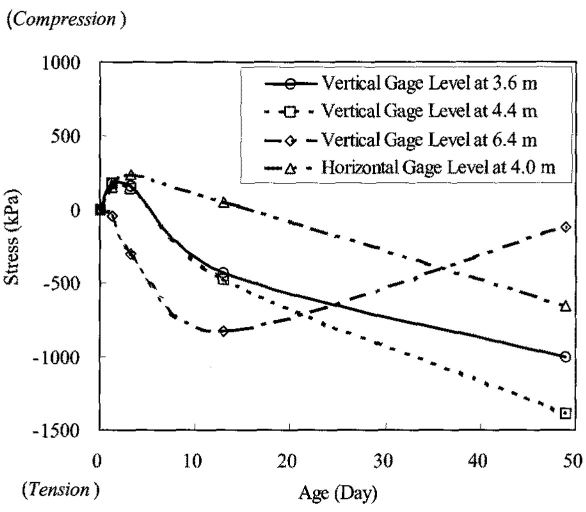

Fig. 15. Residual Stresses for RC Site

addressed to the condition of the rock/shaft interaction based on the results of interface tests described in Nam (2004). The penetration of cement particles into the limestone, which induced outward pressure of concrete on the shaft wall, was caused to develop this negative normal stress at the RC site. This negative normal stress may be caused to develop a higher side resistance. However, the low cohesion value for interface, which induced inward pressure of concrete on the shaft wall, was caused to develop this positive normal stress at HT and DT sites. This positive normal stress may be caused to develop a lower side resistance. These phenomena showed that the residual behavior in the shaft was apparently influenced by the rock/shaft interaction.

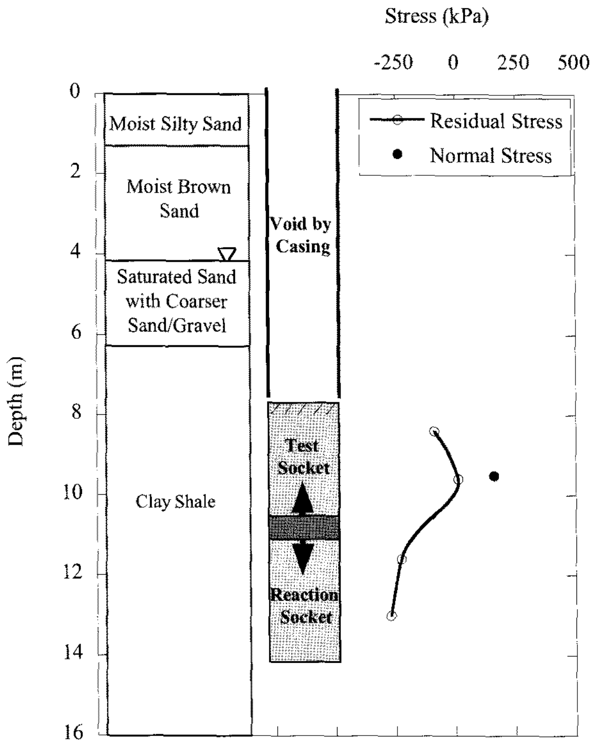

Fig. 16. Residual and Normal Stress at HT Site

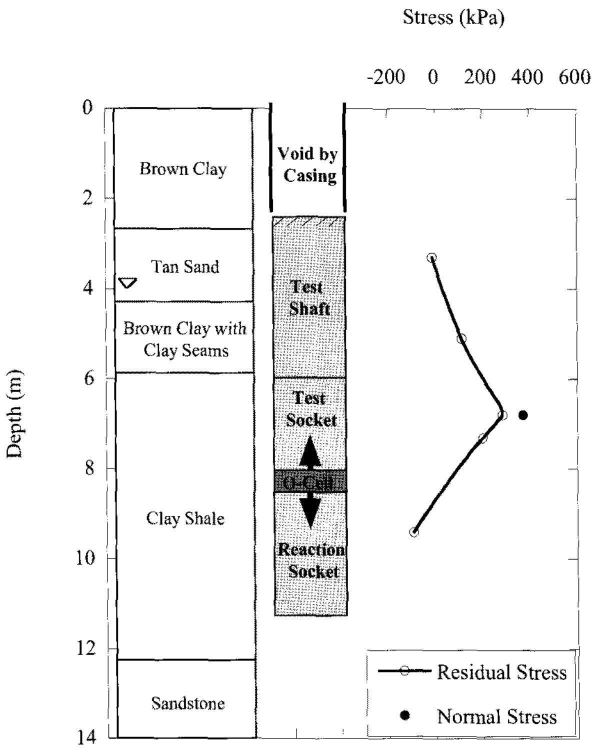

Fig. 17. Residual and Normal Stress at DT Site

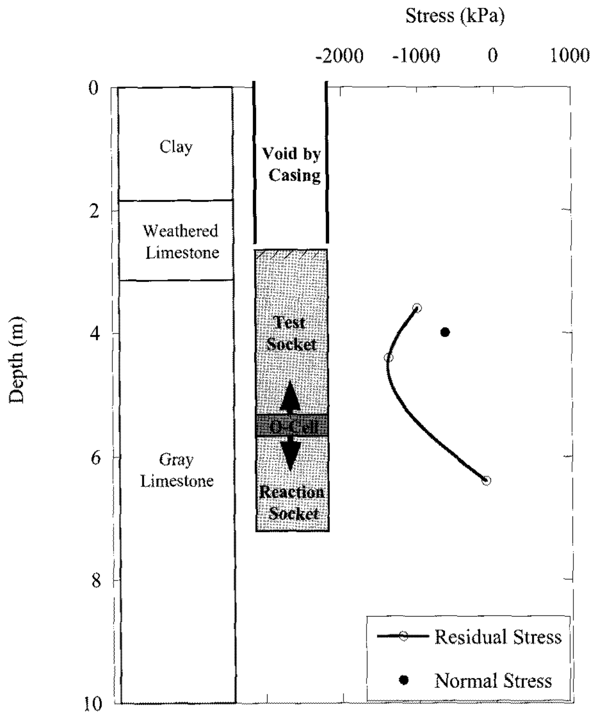

Fig. 18. Residual and Normal Stresses at RC Site

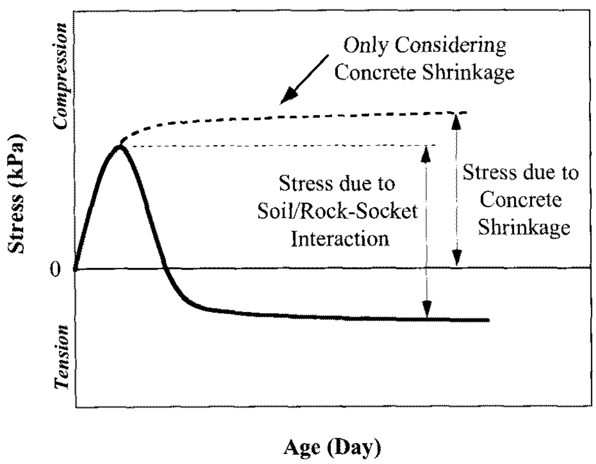

Fig. 19. Proposed Residual Stress Model

5. Summary of Residual Stress Measurements

Based on these various residual behavior after two days and an assumption that the concrete curing behavior of the shaft is uniform along with depth, the residual behavior in the shaft may be controlled to some extent by site conditions (e.g., rock/shaft interaction) as mentioned by Kim et al. (2004). Hence, the residual behavior of shafts in this research was apparently influenced not only by the shrinkage of concrete but also by the rock/shaft interaction. It is not likely that only one phenomenon is present. Rather, both occur simultaneously, with one dominant. Therefore, a residual stress model may be proposed as Figure 19 based on this research.

6. Conclusions

In this study, a field study for residual stresses on rock socketed drilled shafts was conducted in Texas, USA. Based on this field study, the following conclusions are advanced:

(1) A total of three test sites were selected in north central Texas, USA, and a fully instrumented test shaft was installed at each site to measure residual stress.

(2) Residual stresses at the HT site were negative stresses that represented the swelling of the shaft along with the shaft length. The normal stress at the HT site was a positive stress that represented the shrinkage of the shaft along with the shaft diameter. Both residual and normal stresses at the DT site were a positive stress that represented the shrinkage of the shaft in both directions. Both residual and normal stresses at the RC site were negative stresses that represented the swelling of the shaft in both directions.

(3) The penetration of cement particles into the limestone (outward pressure of concrete on the shaft wall) was caused to develop this negative normal stress at the RC site. However, the low cohesion value for interface (inward pressure of concrete on the shaft wall) was caused to develop this positive normal stress at HT and DT sites. These phenomena showed that the residual behavior in the shaft was apparently influenced by the rock/shaft interaction.

(4) Based on these various residual behaviors after two days and an assumption that the concrete curing behavior of the shaft is uniform along with depth, the residual behavior in the shaft may be controlled to some extent by site conditions. Therefore, the residual behavior of shafts in this research was apparently influenced not only by the shrinkage of concrete but also by the rock/shaft interaction. It is not likely that only one phenomenon is present. Rather, both occur simultaneously, with one dominant.

References

1. American Society of Testing and Materials (2000), "Annual Book of ASTM Standards", Vol.4.02, ASTM, West Conshohocken, Philadelphia.
2. Fellenius, B. H. (2002), "Determining The True Distributions of Load in Instrumented Piles", *Proceedings of the International Deep Foundations Congress 2002*, ASCE, Orlando, Florida, pp. 1455-1470.
3. Hayes, J. A., and Simmonds, T. (2002), "Interpreting Strain Measurements from Load Tests in Bored Piles", Proceedings of the Ninth International DFI Conference on Piling and Deep Foundations, Nice, France.
4. Kim, M. G., Cavusoglu, E., O'Neill, M. W., Roberts, T., Yin, S. (2004), "Residual Load Development in ACIP Piles in a Bridge Foundation", *Proceedings of Geo-Support 2004*, ASCE, pp. 223-235.
5. Nam, M. S. (2004), "Improved Design for Drilled Shafts in Rock", Ph. D. Dissertation, Department of Civil & Environmental Engineering, University of Houston, Houston, Texas.

(접수일자 2010. 7. 2, 심사완료일 2010. 12. 28)